

## Antiviral activity of Ribavirin nano-particles against measles virus

Engy M. Ahmed<sup>1</sup>, Samar M. Solyman<sup>2</sup>, Noha Mohamed<sup>3</sup>, Abeer A. Boseila<sup>1</sup>, Amro S. Hanora<sup>2\*</sup><sup>1</sup> National Organization for Drug Control & Research (NODCR), Cairo, Egypt<sup>2</sup> Microbiology & Immunology Department, College of Pharmacy, Suez Canal University, Ismailia, Egypt<sup>3</sup> Biophysics Department, Faculty of Science, Cairo University, 12613 Giza, EgyptCorrespondence to: [ahanora@yahoo.com](mailto:ahanora@yahoo.com)

Received August 17, 2017; Accepted June 26, 2018; Published June 30, 2018

Doi: <http://dx.doi.org/10.14715/cmb/2018.64.9.4>

Copyright: © 2018 by the C.M.B. Association. All rights reserved.

**Abstract:** Measles virus considers an important cause of child morbidity and mortality in some areas as Africa. Ribavirin's activity as a nucleoside analog can disclose the surprisingly broad spectrum action against several RNA viruses under laboratory cell culture conditions. The Current study aimed to investigate the antiviral activity of ribavirin Nano gold particles (AuNPs) against measles virus on vero cell line. Ribavirin- AuNPs was prepared, characterization and the cytotoxicity of ribavirin, AuNPs and ribavirin -AuNPs were tested on vero cells using MTT assay. Antiviral activity of ribavirin, AuNPs and ribavirin- AuNPs were determined on vero cells using simultaneous, pre-infection and post-infection protocols. Results indicated safety of ribavirin and ribavirin-AuNPs on vero cells, there was a reduction by 78.1% when vero cells treated with ribavirin -AuNPs at 99.5µg/ml while, the viral reduction was 25.4% when ribavirin 500 µg/ml was used for the same viral concentration. Our results concluded that ribavirin - AuNPs had a higher antiviral activity with lower dose than ribavirin alone and the maximal activity showed when it used after the virus infection.

**Key words:** Ribavirin; Nano gold particles; Measles virus; Antiviral activity; Vero cell line.

### Introduction

Measles virus (MV), genus *Morbillivirus*, family *Paramyxoviridae*, is an enveloped virus with a non-segmented, negative-strand RNA genome (1). The genomic RNA is encapsidated with the N protein and, together with RNA-dependent RNA polymerase forms a ribonucleoprotein complex (2). It is an infection of the respiratory system, immune system and skin. Measles is unique for infancy rash diseases as it is associated with substantial mortality with a case fatality rate of 5–10% in Africa (3, 4). Immunocompromised hosts, pregnant women, individuals with vitamin A deficiency or poor nutritional status, and individuals at the extremes of age are at increased risk for complications (5).

Despite the availability of effective live vaccines (MMR), measles is still responsible for 4% of mortality in children younger than 5 years of age worldwide (6). In the last decade, the number of measles-related deaths became decreased by more than 90% in all WHO regions, except for South-east Asia (7), and some parts of Africa. Several outbreaks had passed off in 2012 among school children all around the Egyptian governorates and the same case had happened few years earlier in USA at a summer camp (8). Eradication of measles would be a major public health accomplishment and there is no available specific therapeutic remedy according to WHO (2006) (9).

Ribavirin (1-3-D-ribofuranosyl-IH-1, 2, 4-triazole-3-carboxamide) is an antiviral agent that has shown in vitro activity against a broad spectrum of DNA and RNA viruses (10, 11). It exhibits antiviral activity against RNA viruses from the families of paramyxoviruses (12).

The fact that clinical treatment with ribavirin requires high doses with significant side effects (13). The major metabolite of ribavirin is ribavirin-5'-triphosphate (RTP). Erythrocytes concentrate RTP; and they are not efficiently able to dephosphorylate ribavirin. This accumulation of ribavirin is believed to play a role in anemia that has been observed with high-dosage regimens (14, 15, 16). These characteristics of ribavirin had attracted our attention to evaluate its effectiveness against measles virus.

The use of materials in Nano scale allow the modification of the fundamental properties such as solubility, diffusivity, blood circulation half-life, drug release traits, and immunogenicity. Nanostructures can defend drugs encapsulated within them from hydrolytic and enzymatic degradation in the gastrointestinal tract; target the delivery of a drug to various areas of the body for sustained release (17). Gold nanoparticles constitute a category of metallic nanoparticles, which have particular and unique optical, electronic and chemical properties, and high infrared phototherapy potential.

We hypothesize in this study that effect of ribavirin - AuNPs improves the measles virus clearance with lower dose compared to ribavirin alone.

### Materials and Methods

#### Preparation of gold nanoparticles (AuNPs)

The method suggested by J. Turkevich et al. in 1951 and refined by G. Frens in 1970s (18, 19) used in our study, it is simply the reaction between hot Chloroauric acid ( $\text{HAuCl}_4 \cdot 3\text{H}_2\text{O}$ ) and Sodium citrate dehydrate ( $\text{HO}(\text{COONa})(\text{CH}_2\text{COONa})_2 \cdot 2\text{H}_2\text{O}$ , 99%) (Sigma

Aldrich, Germany). Colloidal gold was formed as the citrate ions act as both a reducing agent and a capping agent. Twenty millilitres of 1.0 mM HAuCl<sub>4</sub> were added to 50 ml flask on a stirring hot plate, the solution appeared light yellow, a magnetic stir bar was added inside the flask; the stirring and the temperature were turned on. The solution was brought to boil, 2 ml of a 1% solution of trisodium citrate dehydrate was added to the boiling solution. The gold colloid gradually forms as the citrate was added.

### Preparation of ribavirin loaded gold nanospheres

Five milligrams of ribavirin powder (C<sub>8</sub>H<sub>12</sub>N<sub>4</sub>O<sub>5</sub>) (Roch, Germany, sigma) were dissolved into 10 ml gold nanoparticles (AuNPs) that prepared as described above, suspension was shaken in a dark bottle at 37°C for 24 h. The drug-loaded nanoparticles were separated from the excess drug by centrifugation at 4472 g for 30 min and washed with phosphate buffer saline (PBS) (Biomedicals, France) several times. The free ribavirin contents in solution were calculated from the calibration curve at 225 nm using High performance liquid chromatography (HPLC). The drug loading efficiency was calculated from the following equation:

Loading percentage (%) =

$$\frac{\text{Initial amount of ribavirin} - \text{Supernatant free amount of ribavirin}}{\text{Initial amount of ribavirin}} \times 100$$

### Sample Characterization

#### Transmission electron microscopy (TEM)

Nanoparticles were characterized by their size and morphology using transmission electron microscopy (TEM) (FEI Tecnai G20, Super twin, Double tilt, LaB6 Gun) operating at 200 kV. Samples were prepared for imaging via drying nanoparticles on a copper grid that was coated with a thin layer of carbon. Materials with electron densities that are significantly higher than amorphous carbon are easily imaged. These materials include most metals (e.g., silver, gold, copper, aluminum) (20).

#### Dynamic light scattering (DLS) & Zeta potential measurements

The dynamic light scattering apparatus (Zeta Potential / Particle Sizer NICOMP TM 380 ZLS, USA) was used to measure the size distribution and zeta potential of the prepared AuNPs and ribavirin loaded AuNPs.

#### Visible absorption spectroscopy

The absorption spectra of the prepared AuNPs and ribavirin - AuNPs were measured, using a UV-Vis-IR spectrophotometer (Jenway UV-6420; Barloworld scientific, Essex, UK); at the wavelength range 400-700 nm. Simply a sample is placed between a light source and a photo-detector, and the intensity of a beam of light is measured earlier than and after passing via the sample. These measurements were compared at each wavelength to quantify the sample's wavelength dependent absorption spectrum. The data was typically plotted as absorption versus wavelength. Each spectrum is background corrected using a blank.

### Preparation of vero cell plates

Vero cell line, African green monkey kidney cells

(ATCC: CCL81), was supplied from the Egyptian holding company for vaccines and sera (VACSERA, Egypt). The cell line was originally supplied to VACSE-RA by American type tissue culture collection (ATCC) from which several passages were done and various tissue culture cell line flasks were produced. Vero cells were supplied as 75cm<sup>2</sup> tissue culture flasks and were examined for cell confluence and to ensure absence of contamination using microscope. 1ml of trypsin 2% in PBS (Euro, clone Europe) was added to detach cell line. Detachment assured by examination of flask under microscope. M199E growth media (Biowest, South America) with 10% fetal bovine serum FBS (Biowest-south America) 1% penicillin-streptomycin (Hycolon, USA) was added to the trypsinised cells. Multichannel pipettes (Eppendorf-Germany) were used to transfer 100µl of the suspended cells to 96- tissue culture plates. Plates were left at 37°C, 5%CO<sub>2</sub> incubator overnight until confluent monolayer formed (21, 22).

### Evaluation of the cytotoxicity of ribavirin, AuNPs and ribavirin- AuNPs on vero cells using MTT assay

In order to evaluate the cytotoxic effect of ribavirin, AuNPs and ribavirin- AuNPs on the Vero cells; A colorimetric assay was used, MTT assay. Samples were sterilized and filtered under laminar flow by 0.22µm filter in glass tube and were protected from light. Two-fold serial dilution of each sample in M199E fresh medium containing 2% FBS was added to a confluent monolayer precultured Vero cells plates and incubated for 24h. After overnight incubation, treatment medium was removed from all cells by suction and residual living cells were washed by 200µl PBS twice. About 100µl of MTT (3- [4, 5- dimethyl thiazole- 2-yl]-2, 5 diphenyl tetrazolium bromide) MTT (SERVA, Heidelberg) stained plates were incubated in dark for 4hours. MTT complex crystals were dissolved using 4% acidified isopropanol and were incubated for 15 min. The optical density representing the residual living cells count was measured using microtiter plate reader (Biotek-USA) at wave length 570nm (23, 24). Viability % was measured according to the following equation (25)

$$\text{Viab \%} = (\text{XOD of test samples} / \text{XOD of cell control}) \times 100$$

XOD means average number of wells treated with samples or untreated (control).

The viability was plotted against test product concentration/ dilution and IC<sub>50</sub>% value was presented as the percentage of survived cells compared to control cells and the highest non- toxic dilution was determined (26). IC<sub>50</sub>% was calculated by automated master plex 2010 program.

### Virus strain

Measles virus, Edmonston strain, was kindly obtained from the National Organization for Research and Control of Biologicals (NORCB); Virus titers used as 4.679 log<sub>10</sub> / ml.

### Simultaneous treatment of virus with ribavirin and ribavirin- AuNPs

Effect was calculated based on the log difference between virus titer treated with samples and virus titer

of control non-treated ( $\Delta$ log 10 TCID<sub>50</sub>/ml) (27). Equal amount of the 1000CCID<sub>50</sub>/ml of the measles virus with 1/20(500 $\mu$ g/ml) of ribavirin was mixed together / 1000CCID<sub>50</sub>/ml of the measles virus with 1/20(99.5 $\mu$ g/ml) of ribavirin- AuNPs also was mixed together and was incubated at 37°C for 1h, then tenfold dilution of samples was done on previously seeded monolayer sheet of vero cells (prepared 24 hours before the experiment as described above). Negative control and virus control were included in each sample plates. Cells were observed for cytopathic effect (CPE) daily until extensive CPE effect (75-100%) of monolayer cell. After 5-7 days when the virus control showed extensive CPE, each dilution was collected and stored frozen. Each dilution with the virus control was subjected to back titration to ensure the drop in the virus titer compared to the control (28). Number of cells showed CPE were recorded and those did not as well. Virus titer was calculated using the method described by (29) as follows:

50% endpoint (TCID<sub>50</sub>) = (percentage of CPE >50% - 50) / (percentage of CPE >50% - percentage of CPE <50%)  $\times$  log dilution.

where “>50%” dilution is the last dilution expressed for which  $\geq$  50% wells display CPE, (“Above 50%” and “Below 50%” values are fraction of wells with CPE at the last dilution for which  $\geq$ 50% wells display CPE and fraction of wells with CPE at the next dilution, respectively.

The difference between the virus titer of control and treated virus was calculated and depletion rate was measured as the percentage loss in the virus titer.

#### **Pre-infection treatment of virus with ribavirin and ribavirin- AuNPs on vero cells**

Two-fold serial dilution of ribavirin and ribavirin-AuNPs was applied on previously seeded cell monolayer (prepared 24 hours before the experiment as described above) and incubated at 37°C for 90 min. Virus suspension 1000CCID<sub>50</sub>/ml was added to each well of the treated cell monolayer (100 $\mu$ l/well), incubated at 37°C for 5-7 days. The presence of (75%- 100%) CPE in virus infectivity control cultures was confirmed. Back titration was done to evaluate the drop in virus titer (28). Negative control and virus control were included in each sample plates. Pre-infection effect was calculated based on the log difference between virus titer treated with samples and virus titer of control non-treated as virus titer was calculated using the method described by (29).

#### **Evaluation of the post- infection treatment of ribavirin and ribavirin- AuNPs against measles virus in vero cells**

A virus suspension 1000CCID<sub>50</sub>/ml was pre-incubated with vero cell plates (prepared 24 hours before the experiment as described above) for 90 min; then Two-fold serial dilution of ribavirin and ribavirin AuNPs were added to the infected cell monolayer. The incubation was done for 5-7 days at 37°C. The presence of (75%- 100%) CPE in virus infectivity control cultures was confirmed, back titration was done to evaluate the post-infection treatment of ribavirin and ribavirin -AuNPs against measles (28). Negative control and virus control were included in each sample plates. Antiviral

activity was calculated using the method described by (29).

Comparative evaluation was processed to measure the average loss of the virus titer as percentage loss(%depletion rate) which reflecting the antiviral potential of ribavirin and ribavirin- AuNPs on treated Vero cells compared to only virus treated cells.

#### **Quantification of measles virus using Real time reverse transcriptase polymerase chain reaction (qRT-PCR)**

##### *Viral RNA extraction*

From simultaneous, pre-infection and post-infection treatment plates of ribavirin and ribavirin-AuNPs experiments, Viral RNA was extracted from vero cells infected with measles virus when syncytia involved at least 75%. Growth medium was removed from the infected plates, the cells were rinsed once with PBS and PBS was discarded. To detach the cells, 100 $\mu$ l of trypsin were added in each well. The cells were incubated for 20-30 min, transferred to a micro centrifugation tubes and pelleted by centrifugation for 5 min at 2500g. RNA was extracted using Gene JET viral RNA kit (thermo-fisher, Germany), 200 $\mu$ l of lysis buffer were added and stored at -80°C until use (according to the manufacturer instructions). The purified RNA for downstream applications was used and stored RNA at -20°C or -70°C until use. The yield of total RNA obtained was determined spectrophotometrically at 260 nm.

##### *Primer selection*

Primer sequence for the studied target gene was used for amplification of 450 nucleotides corresponding to the COOH terminal 150 amino acids of the N protein which was the most conserved region. Forward and reverse primers were used from a previous publication (30).

##### *Quantitative (qRT-PCR) assay*

To assess the linearity of the quantitative real-time RT-PCR, 10-fold serial dilutions were prepared (10<sup>7</sup>-10<sup>1</sup> copies) of cDNA of measles control viral RNA, measured using primers of their N gene. RNA extracted from the infected cells (1000ng) was used in each 20 $\mu$ l real time RT-PCR reaction. RT-PCR reactions were performed in triplicate in a Micro Amp optical 96-well reaction plate (Applied Biosystem) using reagents supplied in SensiFAST™ SYBR® Hi-ROX One-Step Kit (Bioline, UK). The prepared reaction mix samples were applied in real time PCR (Step One Applied Biosystem, Foster city, USA). Thermocycling parameters included a reverse transcription step at 45°C for 10 min, following by DNA polymerase activation at 95°C for 2 min and 40 PCR cycles of 95°C for 5s/ 60°C for 10s and 72°C for 5s.

##### **Statistical analysis**

All results were expressed as mean  $\pm$  SEM and analyzed using Statistical Package for Social Sciences (SPSS) software package version 16 (Chicago, USA). Statistical significance was tested using one-way analysis of Variance (ANOVA) followed by Bonferroni post hoc comparisons to test the significance difference among the group means. Data was considered statisti-

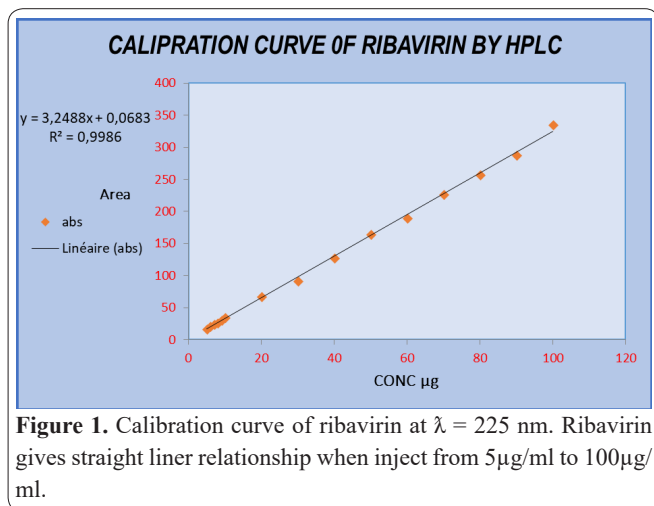


**Figure 1.** Calibration curve of ribavirin at  $\lambda = 225$  nm. Ribavirin gives straight liner relationship when inject from  $5\mu\text{g/ml}$  to  $100\mu\text{g/ml}$ .

cally significant with  $P \leq 0.05$ .

## Results

### Preparation of ribavirin loaded gold Nano-spheres

Conversion of gold from yellow to wine red indicates formation of gold Nano particles (AuNPs) and conversion of AuNPs from wine red to blue indicate good encapsulation of ribavirin on AuNPs as it reflect increasing in size of AuNPs due to loading of ribavirin, from calibration curve of ribavirin (Figure 1) and the equation, we found that Loading percentage% was 39.8% so loading amount of ribavirin was  $199\mu\text{g/ml}$ .

### Sample Characterization

#### Transmission electron microscopy

From the TEM measurements, the gold nanoparticle was found to be spherical with an average diameter of 15 nm (Figure 2 a, b). TEM imaging had significantly higher resolution (by a factor of about 1000) than light-based imaging techniques which giving morphological examination with direct visualization. Amplitude and phase variations in the transmitted beam provide imaging contrast that is a function of the sample thickness (the amount of material that the electron beam must pass through) and the sample material (heavier atoms scatter more electrons and therefore have a smaller electron mean free path than lighter atoms).

#### Dynamic light scattering (DLS)

The resulted measured mean diameters of AuNPs and ribavirin - AuNPs were  $14.54 \pm 2.4$  nm and  $28.65 \pm 5.2$  nm, respectively (Figure 3 a, b). This increase in diameter from 14.54 nm to 28.65 means that ribavirin drug make a hydrodynamic layer around gold nanoparticles and in turn that mean a successful loading of

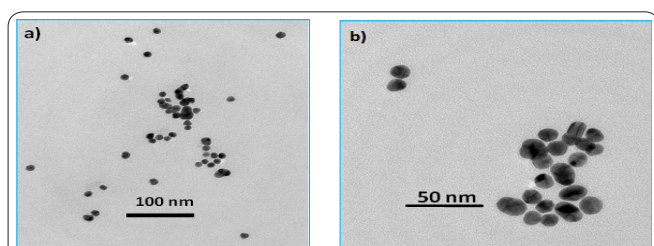


**Figure 2.** TEM images of AuNPs. a: scale bar 100 nm. b: scale bar 50 nm.

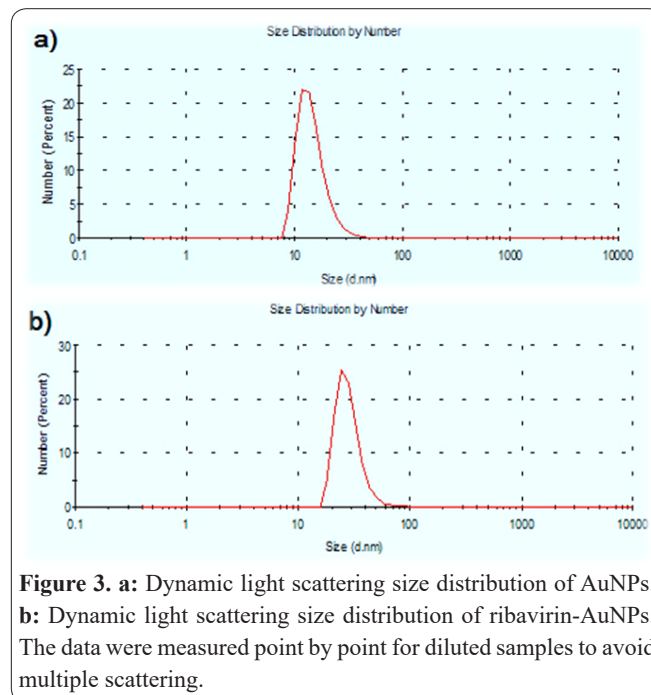


**Figure 3. a:** Dynamic light scattering size distribution of AuNPs. **b:** Dynamic light scattering size distribution of ribavirin-AuNPs. The data were measured point by point for diluted samples to avoid multiple scattering.

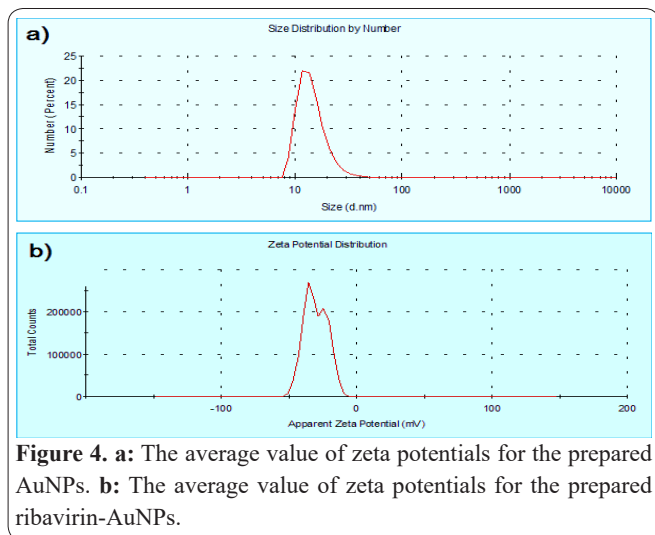
drug on nanoparticles. As particle size affects the drug release and is a critical parameter of characterization so using dynamic light scattering to determine the particle size distribution of AuNPs and ribavirin – AuNPs is a critical tool in our characterization. As it is give a description of the particle's motion in the medium, measuring the diffusion coefficient of the particle and using the autocorrelation function (20, 31). It is extensively used to determine the size of Brownian nanoparticles in colloidal suspensions in the Nano range (20). Shining monochromatic light (laser) onto a solution of spherical particles in Brownian motion caused a Doppler shift when the light hits the moving particle, changing the wavelength of the incoming light. So, increase in diameter of AuNPs when ribavirin loaded means that ribavirin drug make a hydrodynamic layer around gold nanoparticles and in turn that mean a successful loading of drug on nanoparticles.

#### Zeta potential measurements

The average zeta potential of the prepared AuNPs was -38 mv. The average zeta potential of ribavirin loaded AuNPs was -30.3 mv. This decrease in negativity indicates a successful loading of drug (figure 4 a, b). As these negative values indicates moderate degrees of stability of the prepared nanoparticles. Negative value arises due to negative charge of citrate ions that act as capping agent around colloidal gold. It considered a critical tool for understanding the state of the nanoparticle surface and predicting the long-term stability of them. Zeta potential can also provide information regarding the nature of material coated onto the surface of nanoparticles (32).

#### Visible spectroscopy

The Plasmon band observed for the wine red colloidal gold at 525nm are pertaining to Au colloids and 225nm is characteristic to pure ribavirin. The addition of ribavirin decreases the intensity steadily with time with appearance of another peak at 650 nm (Figure 5). The appearance of the new peak is due to the aggrega-



tion of gold nanoparticles leading to the formation of gold-drug complex. Abdelhalim MAK, et al (33) stated that Nanoparticles made from certain metals, such as gold, strongly interact with specific wavelengths of light and the unique optical properties of these materials is the foundation for the field of plasmonics.

**Evaluation of the cytotoxicity of ribavirin, AuNPs and ribavirin- AuNPs against vero cells using MTT assay**

From cytotoxicity assay it was revealed that AuNPs, ribavirin and ribavirin - AuNPs were safe at all dilutions/ concentrations we used as no detachment cell (table 1). As the initial concentration we used were 260, 1000, 199µg/ml of AuNPs, ribavirin and ribavirin- AuNPs respectively from which two-fold dilution were used. Calculation of IC50 which defined as concentration of drug that gives half- maximum response, the 50% effective response were 464, 1025 and 215 for AuNPs, ribavirin, and ribavirin- AuNPs respectively as they re-

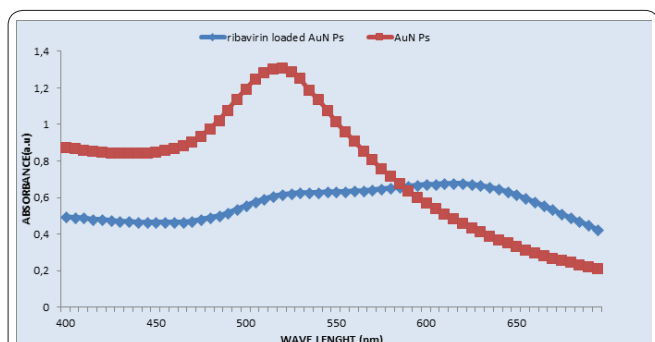


**Figure 5.** The absorption spectrum of the prepared AuNPs and ribavirin - AuNPs. As red line is a characteristic absorbance peak of Nano gold particle at  $\lambda = 525\text{nm}$ . Blue line represents decrease of intensity to  $\lambda = 650\text{nm}$  due to loading of ribavirin on Nano gold particles

**Table1.** Cytotoxicity of Ribavirin, AuNPs and Ribavirin- AuNPs.

Concentration of Ribavirin (µg/ml)	Concentration of AuNPs (µg/ml)	Concentration of Ribavirin – AuNPs (µg/ml)	Cytotoxicity%
1000	260	199	0%
500	130	99.5	0%
250	65	49.75	0%
125	32.5	24.87	0%

present the highest non-toxic concentration we can use . The recorded data was generated using averaged optical density (O.D) reading for the control cells and the average O.D reading for samples that were measured at 570nm using microplate reader.

**Morphological changes post cell treatment**

Microscopic examination of treated cells revealed that ribavirin, AuNPs and ribavirin- AuNPs were safe on vero cells when used in the highest concentrations compared to untreated control (Figure 6b), where vero cell showed well adherence, homogenous distribution in the culture field (Figure 6 a).

**Simultaneous, pre-infection and post-infection treatment of measles virus with ribavirin and with ribavirin-AuNPs on vero cell line**

According to our calculation of the end point dilution from Reed- Muench equation We found that there is 1.32, 1.72 and 2.25 log difference between virus treated simultaneously, pre-infected and post-infected respectively with 1/20 (99.5µg/ml) ribavirin- AuNPs and virus control (untreated) as untreated cells was infected with tenfold serial dilution of virus suspension and incubated at 37°C for 5- 7 until extensive CPE observed. and 0.536, 0.7 and 1.1 log difference between virus that treated simultaneously, pre-infected and post-infected respectively with 1/20 (500µg/ml) ribavirin and virus control (untreated). Experiments were done as three independent assays for each sample, were high non-toxic concentration of each sample was used. CPE induced by measles virus observed under the microscope after 5–7 days.

The depletion rate of measles virus by ribavirin and ribavirin -AuNPs had variability based on experiment technique as post-infection showed the best inhibitory activity of both ribavirin and ribavirin - AuNPs with depletion rate was 27.5% and 56.25% respectively. Pre-infection showed inhibitory activity of both ribavirin and ribavirin - AuNPs with reduction in virus titer by 17.5% and 43% respectively. Where simultaneous treatment showed the lowest inhibitory activity of both ribavirin and ribavirin – AuNPs comparing with two other

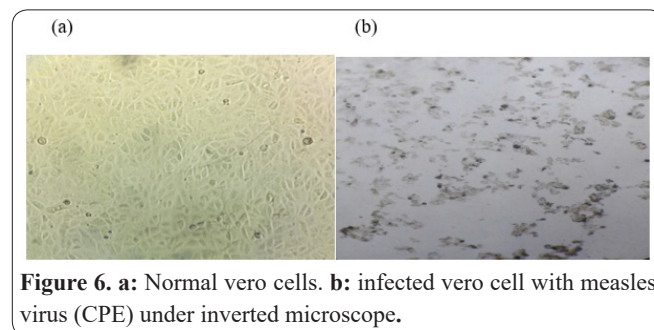
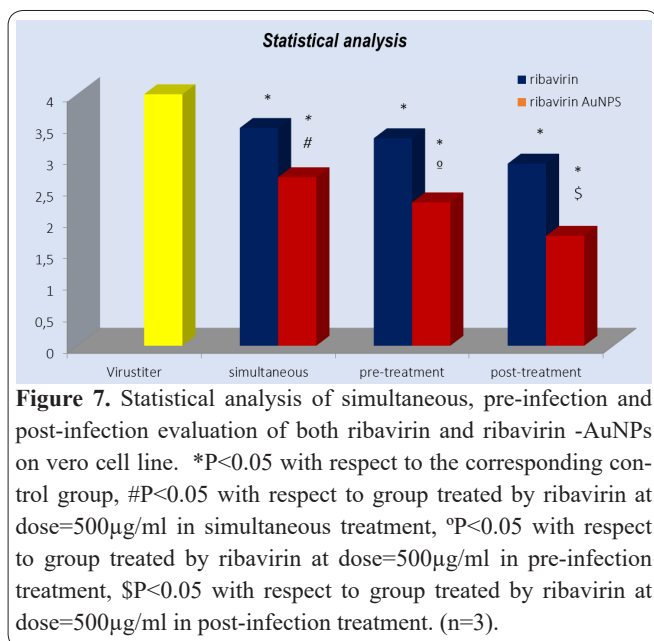


**Figure 6. a:** Normal vero cells. **b:** infected vero cell with measles virus (CPE) under inverted microscope.



experiments as loss in measles virus titer was 13.4% and 33% respectively. In all experiments, treatment of ribavirin and ribavirin- AuNPs showed that ribavirin-AuNPs have induced inhibition of 1000TCID<sub>50</sub>/ml of measles virus at 99.5µg/ml more than ribavirin alone when used at 500µg/ml. Also higher dilution of ribavirin - AuNPs were more active than ribavirin at 500µg/ml. Our results confirmed our suggestion that ribavirin -AuNPs had inhibitory effect more significant than ribavirin with lower dose (figure 7).

#### Quantification of measles virus using real time reverse transcriptase polymerase chain reaction (qPCR)

Using ribavirin at concentrations 500, 250 and 125µg/ml resulted in different results depending on technique of application of drug on vero cells as it had almost similar effect on entry of virus (10.9%) and in prophylacting (9.9%) against measles infection. In application of ribavirin after virus infection we observed higher activity (22.5%). In all tests ribavirin inhibitory activity not exceed 30% at higher concentration 500µg/ml, but ribavirin - Au NPs showing inhibitory activity against virus in antiviral treatment that exceed 70% at highest concentration 99.5µg/ml and at lowest concentration 24.8µg/ml it had inhibitory activity more than 50%. Ribavirin - Au NPs resulted on considered loss of virus titer in all tests. And unlike ribavirin it had different activity in entry of virus (56.5%) and in prophylaxis activity (32.3%). Surprisingly it had activity in inhibition of simultaneous action more than pre-infection action unlike ribavirin. We observed that the action in inhibition of virus infection was due to action of ribavirin that have action on virus from entry until replication but with different degree as the most effective action is during replication with modest effect on entry and as prophylacting agent from infection (figure 8).

Our estimates of ribavirin- AuNPs effectiveness against measles virus on Vero cells suggest that the gold Nano particles provides excellent activity to ribavirin by increase in surface area and dominance of quantum effects which is associated with very small sizes and large surface area to volume ratio (34). The observa-

tion of ribavirin-AuNPs activity at lower concentrations than ribavirin even with enhancing viral clearance is a cause for concern because this may decrease the diverse effect associated with high dose regimen of ribavirin. Because most recent research indicated that accumulation of ribavirin in erythrocytes is responsible for haemolytic anemia (16).to minimize this risk, ribavirin -AuNPs administration was suggested for further trials to improved and maintained.

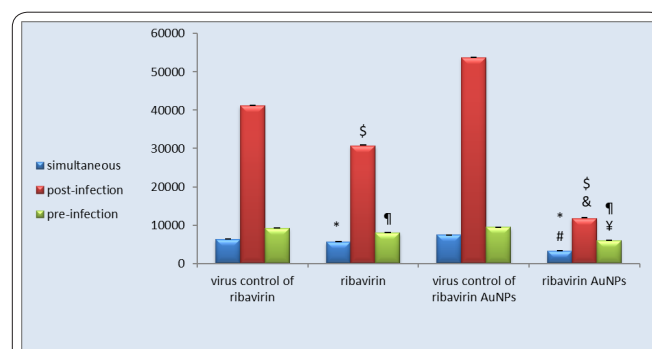
#### Discussion

Measles virus standing as number one killer of young children as one third of children were trap infection in the first and second years, and most other children catch infection before age 5 years (35, 36, 37).

Some studies reported the ability of using oral and intravenous ribavirin against measles infections (38, 39). Additionally Hosoly *et al* (40) determined that ribavirin inhibited the replication of Subacute sclerosing panencephalitis (SSPE) greater than other nucleoside and non-nucleoside compounds. As it is a serious complication of persistence of measles virus in brain (41). Ribavirin had been used to aid in recovery from severe measles pneumonia, although their exact clinical efficacy is still unproven (39, 37). Indeed due to the required large daily doses of ribavirin to sustain a beneficial response due to renal clearance and to maintain the sustained virologic response (SVR) (42), the foremost toxicity associated with ribavirin is a dose-dependent hemolytic anemia, which takes place in about 50% of individuals administered ribavirin, resulting in a ribavirin dose reduction (43).

Current study used gold Nano-particles due to it is unique properties as a carrier molecules as Some studies advocate that coupling of ribavirin to a carrier molecule offers the potential of a therapeutic with improved safety and efficacy by targeting drug delivery of ribavirin to key tissues inflamed at the same time as preventing the hemolytic anemia that is resulting in exposure of red blood cells to ribavirin.

J. Turkevich (18) approach was used as it is the primary and simplest technique ever used for preparation



of Nano particles which causes Au<sup>3+</sup> ions to be reduced to neutral gold atoms. Actually Ribavirin was successfully loaded on AuNPs and it was confirmed by characterization of both AuNPs and ribavirin - AuNPs by using TEM imaging, DLS, and Zeta potentials as Nanoparticles with Zeta Potential values greater than +25 mV or less than -25 mV typically have high degrees of stability. UV-visible absorption spectroscopy was used for characterization as the optical properties are sensitive to size, shape, concentration, and refractive index of nanoparticles. For small monodisperse gold nanoparticles the surface plasmon resonance phenomena (SPR) causes an absorption of light within the blue-green portion of the spectrum (~450 nm) whilst red light (~700 nm) is reflected, yielding a wealthy red color. As particle size increases, due to loading of ribavirin the wavelength of surface plasmon resonance related absorption shifts to longer. Red light is then absorbed, and blue light is reflected.

Current study proved safety of ribavirin and ribavirin- AuNPs on vero cell line by evaluated cytotoxicity using cell culture models. MTT assay was used as it has several benefits as it is easy to perform, the assessments are objective, it could be computerized and the cytotoxicity assessment may be made in parallel with antiviral activity evaluation (23, 44, 45). It depending on conversion of MTT yellow solution into purple formazan crystals by living cells mitochondrial enzymes as conversion of color was directly related to number of viable cells.

Vietinck & Vanden-Berghe (46) reported that numerous cell culture assays are available and may be successfully applied for the antiviral assessment of synthetic or natural compounds, one among them is visual quantitation of antiviral activity of the virus triggered cytopathic effect (CPE) (47, 48, 49). For measles virus as it induce CPE in cells, visual scoring of CPE inhibition is performed more frequently because it is rapid, and permits a number of compounds to be evaluated collectively using 96-well micro plates (50).

In the current study we used TCID<sub>50</sub> titration method which based on the end-point dilution of the virus at which a cytopathic effect (CPE) is detected in at least 75% of the cell culture replicates infected by a given amount (1000CCID<sub>50</sub>/ml) of measles virus suspension (29). Comparative evaluation was processed to measure the average loss of the virus titer as percentage loss (%depletion rate) which reflecting the antiviral potential of ribavirin and ribavirin- AuNPs on treated Vero cells compared to only virus treated cells (figure 9).

In 2016, Ortac Ersoy (51) reported that ribavirin and high-dose vitamin A might be a treatment option in addition to supportive treatment in complicated adult measles cases. Our finding showed that both ribavirin and ribavirin-AuNPs resulted in noticeable loss in virus infectivity titer. Current results showed that the maximum inhibitory effect of both ribavirin and ribavirin-AuNPs was in post-infection treatment. It may explained as the mechanism of action of ribavirin is due to inhibition of function of virus-coded RNA polymerase necessary to initiate and elongate viral mRNA which inhibited virus replication after virus infection (52).

In 2007 Thomas *et al.* (53) developed a quantifica-

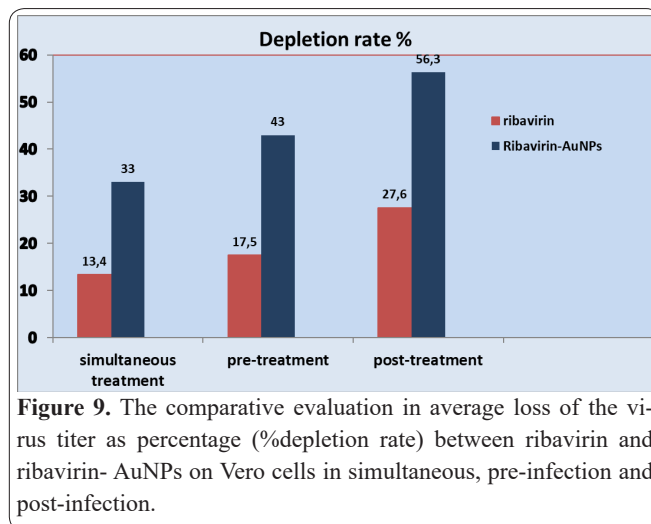


**Figure 9.** The comparative evaluation in average loss of the virus titer as percentage (%depletion rate) between ribavirin and ribavirin- AuNPs on Vero cells in simultaneous, pre-infection and post-infection.

tion assay for detection of haemagglutinin (H) gene in measles virus using a real-time PCR method, similarly Hummel *et al* in 2006 (54) developed a method targeting multiple genes of measles virus. In both methods, the sensitivity limits were two and ten copies per reaction, respectively (53, 54). Our finding showed a representative linear standard curves using control viral RNA (from 10<sup>1</sup> to 10<sup>7</sup> copies per reaction) (figure10) suggested that the reliable measurement range of our assay is (10<sup>1</sup>-10<sup>7</sup>) copies per reaction. Our values were very close to those of Thomas and Hummel methods, even though the target gene and/or region of measles virus were different. Taken together, the results suggest that our method is sensitive, quantitative for the measles virus N gene, and is applicable to the quantification of measles virus as we used N gene as it is the most abundant structure polypeptide and highly conserved (55, 56).

qPCR data, confirmed cell culture results as ribavirin and ribavirin - AuNPs had decreased the virus titer of treated cells than control with significant difference P<0.05 and ribavirin - AuNPs was more effective than ribavirin. There was a direct relationship between concentration and inhibitory effect of ribavirin on measles virus titer on cell culture.

In agreement with these results, we concluded that ribavirin -AuNPs had more potent effect on reduction of virus titer more than ribavirin as Nanoparticles enhance activity of ribavirin and reduce dose required. The changes in properties of ribavirin will be due to increase

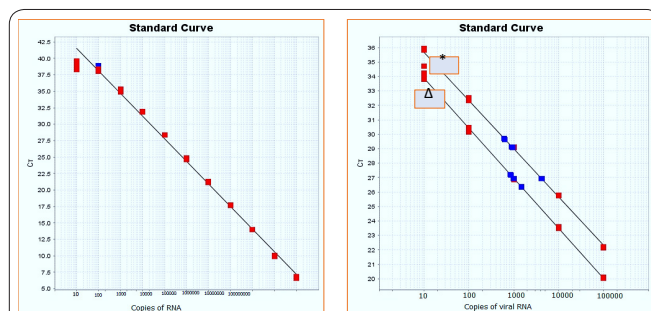


**Figure 10.** A representative standard curve using the standard measles control viral RNA for (a) simultaneous effect, (b) for pre - treatment (Δ) and post - treatment (\*), as the x - axis indicated the logarithmic concentration (log<sub>10</sub>) of the viral RNA and y - axis indicates the Ct value red and blue dots represent virus control of ribavirin and ribavirin - AuNPs respectively.

in surface area and dominance of quantum effects which is associated with very small sizes and large surface area to volume ratio (34). Ribavirin-AuNPs had better activity against measles virus when used post-infection which supports its use in treatment of measles infection, its higher antiviral activity in the pre-infection protocol might also suggest its use as a prophylactic agent during outbreaks to limit spread of infection. Our study suggests the use of ribavirin-AuNPs for the treatment of measles infections and recommends more *in vivo* studies to demonstrate the reduction of the side effects with the reduction of dose.

Our study indicated that both ribavirin and ribavirin-AuNPs had antiviral activity against measles virus as we hypothesized and using gold Nano particles enhance antiviral activity and viral clearance. We predicted that ribavirin and ribavirin – AuNPs will be higher in post treatment than pre- treatment and finally, simultaneous treatment. However, ribavirin- AuNPs contrary to this hypothesis as it had higher activity in simultaneous than pre- treatment which requires more analysis to understand this phenomenon.

### Acknowledgments

The authors thank Dr. Dina Sabry Abdel Fatah, Faculty of Medicine, Cairo University, for her valuable assistance with the quantification of PCR.

The work was supported by National Organization of Drug Control & Research.

### Conflict of interest

The authors do not have any commercial associations that might create a conflict of interest in connection with the manuscript.

### Author contribution

Engy Mahmoud: designed and carried out all experimentation and drafted the manuscript.

Dr. Noha: participated in preparation and characterization of nanoparticles.

Dr. Abeer Boseila: participated in experimental design and preparation of cell line assay.

Dr. Samar Solymann & Dr. Amro: assisted in experimental design, writing and review.

### References

- Griffin, D.E. Measles virus. In *Fields Virology*,. In Edited by D. M. Knipe, P.M.H., D. E. Griffin, R. A. Lamb, M. A. Martin, B. Roizman & S. E. Straus. (ed), Philadelphia: Lippincott Williams & Wilkins 2001.
- Cathomen T, Mrkic B, Spohner D, Drillien R, Naef R, Pavlovic et al, A matrix-less measles virus is infectious and elicits extensive cell fusion: consequences for propagation in the brain . *The EMBO journal* 1998; 17: 3899-3908.
- Nandy R, Handzel T, Zaneidou M, Biey J, Cuddy R.Z, Perry R et al. Case-fatality rate during a measles outbreak in eastern Niger in 2003. *Clin. Infect. Dis.: an official publication of the Infectious Diseases Society of America* 2006; 42: 322-328.
- Grais R.F, Dubray C, Gerstl S, Guthmann J.P, Djibo A, Nargaye K.D et al. Unacceptably high mortality related to measles epidemics in Niger, Nigeria, and Chad. *PLoS medicine* 2007; doi: 10.1371/journal.pmed.0040016. 4: e16.
- Moss W.J. & Griffin D.E. Measles. *Lancet* (London, England)

2012; 379: 153-164.

6. Bryce J, Boschi-Pinto C, Shibuya K. & Black R.E. WHO estimates of the causes of death in children. *Lancet* (London, England) 2005; 365: 1147-1152.

7. Strebel P.M, Cochi S.L, Hoekstra E, Rota P.A, Featherstone D, Bellini W.J. et al. A world without measles. *J INFECT DIS* 2011; doi: 10.1093/infdis/jir111.204 Suppl 1: S1-3.

8. Barskey A.E, Glasser J.W. & LeBaron C.W. Mumps resurgences in the United States: A historical perspective on unexpected elements. *Vaccine* 2009; 27: 6186-6195.

9. World Health Organization. Global distribution of measles and rubella genotypes--update. *Wkly Epidemiol Rec* 2006; 81: 474-4

10. Crumpacker C.S. Overview of ribavirin treatment of infection caused by RNA viruses. In R. A. Smith, V. Knight, and J. A. D. Smith (ed.), *Clinical applications of ribavirin*. Academic Press, Inc., New York 1984; 33-37.

11. Sidwell R.W. *In vitro* and *in vivo* inhibition of DNA viruses by ribavirin, In R. A. Smith, V. Knight, and J. A. D. Smith (ed.), *Clinical applications of ribavirin*. Academic Press, Inc., New York 1984; 19-32.

12. Hruska J.F, Bernstein J.M, Douglas R.G, Jr. & Hall C.B. Effects of ribavirin on respiratory syncytial virus *in vitro*. *Antimicrob. Agents Chemother.* 1980; 17: 770-775.

13. Cummings K.J, Lee S.M, West E.S, Cid-Ruzafa J, Fein S.G, Aoki Y et al. Interferon and ribavirin vs interferon alone in the re-treatment of chronic hepatitis C previously nonresponsive to interferon: A meta-analysis of randomized trials. *Jama* 2001; 285: 193-199.

14. Shulman N.R. Assessment of hematologic effects of ribavirin in humans. In R. A. Smith, V. Knight, and J. A. D. Smith (ed.), *Clinical applications of ribavirin*. Academic Press, Inc., New York 1984; 79-92.

15. McCormick J.B, King I.J, Webb P.A, Scribner C.L, Craven R.B, Johnson K.M et al. Lassa fever. Effective therapy with ribavirin. *N. Engl. J. Med.* 1986; 314: 20-26.

16. Homma M, Matsuzaki Y, Inoue Y, Shibata M, Mitamura K, Tanaka N. et al. Marked elevation of erythrocyte ribavirin levels in interferon and ribavirin-induced anemia. *Clin. Gastroenterol. Hepatol.* The official clinical practice journal of the American Gastroenterological Association 2004; 2: 337-339.

17. Nimesh S, Manchanda R, Kumar R, Saxena A, Chaudhary P, Yadav V, et al. Preparation, characterization and *in vitro* drug release studies of novel polymeric nanoparticles. *Int. J. Pharm* 2006; 323: 146-152.

18. Turkevich J, Steenson P.C, Hillier J, "A study of the nucleation and growth processes in the synthesis of colloidal gold". , *Discuss. Faraday. Soc* 1951; 11: 55-75.

19. Frens G. "Particle size and sol stability in metal colloids". *Colloid Polym Sci* 1972; 250: 736-741.

20. Pal S.L, Jana U, Manna PK, Mohanta G.P, & Manavalan. "Nanoparticle: An overview of preparation and characterization" *Int. J. Appl. Pharm. Sci. Res* 2011; 1: 228-234.

21. Yasumura Y & Kawakita Y. Studies on SV40 in tissue culture – preliminary step for cancer research “*in vitro*”. Article in *Japanese* 1963; 21: 1201-1215.

22. Cote R.J. Aseptic technique for cell culture. *Curr Protoc Cell Biol* 2001; Chapter 1, Unit 1.3.

23. Takeuchi H, Baba M. & Shigetani S. An application of tetrazolium (MTT) colorimetric assay for the screening of anti-herpes simplex virus compounds. *J. Virol. Methods* 1991; 33: 61-71.

24. Sieuwerts A, Klijn J.G.M, Peters H.A, Foekens J.A. The MTT tetrazolium salt assay scrutinized: how to use this assay reliably to measure metabolic activity of cell cultures *in vitro* for the assessment of growth characteristics, IC50 – values and cell survival. *Eur*

J Clin Chem Clin Biochem 1995; 33: 813-823.

25. Chen T.h, kutty P. & Lowe L.E. Measles outbreak associated with an international youth sporting event in the united states 2007. *Pediatr. Infect. Dis. J* 2010; 29: 794-800.

26. Marini A.M, Ahmed I.B, Yahya M.D. & Yamin B.M. Optimization of cytotoxicity assay for estimating CD50 values of plant extracts and organometallic compounds. *Malays Appl Biol* 1998; 27: 63-67.

27. Ogutcu H, Sokmen A, Sokmen M, Polissiou M, SerKedjjeva J, Daferera D, et al. Bioactivities of the Various Extracts and Essential Oils of *Salvia Limbata* C.A. Mey. And *Salvia sclarea* L. *Turk. J. Biol.* 2008; 32: 181-192.

28. Dragana S, Dragana M.C, Branka V.G, Draga S & Jelena K.V. Evaluation of antiviral activity of fractionated extracts of *saga salvia officinalis* L. (Lamiaceae). *Arch.Biol.Sci. Belgrade* 2008; 60: 421-429.

29. Reed J. & Muench H. simple method of estimating fifty percent endpoints. *Am J Hyg* 1938; 27: 493-494?

30. KoruKluoglu G, Liffick S, Guris D, Kobune F, Rota A.P, Bellini J.W et al. Genetic characterization of measles virus isolated in turkey during 2000-2001. *Virol. J.* 2005; 2: 58.

31. DeAssis D.N, Mosqueira V. C, Vilela J.M, Andrade M.S. & Cardoso V.N. "Release profiles and morphological characterization by atomic force microscopy and photon correlation spectroscopy of 99m Technetium – fluconazole Nano capsules" *Int J Pharm*, 2008; 349: 152 – 160.

32. Pangi Z, Beletsi A & Evangelatos K. "PEG-ylated nanoparticles for biological and pharmaceutical application". *Adv. Drug Deliv. Rev* 2003; 24: 403- 419.

33. Abdelhalim M.A.K, Mady M.M, & Ghannam M.M. Physical Properties of Different Gold Nanoparticles: Ultraviolet-Visible and Fluorescence Measurements. *J Nanomed Nanotechnol* 2012; 3: 133.

34. Williams D. The relationship between biomaterials and nanotechnology. *Biomaterials* 2008; 7: VoL. 193, 1515–1526.

35. Foege W.H. & Foster S.O. Multiple antigen vaccine strategies in developing countries. *Am. J. Trop. Med. Hyg.* 1974; 23: 685-689.

36. Halsey N.A, Boulos R, Mode F, Andre J, Bowman L, Yaeger R.G, et al. Response to measles vaccine in Haitian infants 6 to 12 months old. Influence of maternal antibodies, malnutrition, and concurrent illnesses. *N. Engl. J. Med.* 1985; 313: 544-549.

37. Pal G. Effects of ribavirin on measles. *J Indian Med Assoc* 2011; 109: 666-667.

38. Banks G. & Fernandez H. Clinical use of ribavirin in measles: a summarized review. In R. A. Smith, V. Knight, and J. A. D. Smith (ed.), *Clinical applications of ribavirin*. Academic Press, Inc., New York, 1984; 203-209.

39. Forni A.L, Schluger N.W. & and Roberts R.B. severe measles pneumonia in adults: an evaluation of clinical characteristic and therapy with intravenous ribavirin. *Clin. Infect. Dis.* an official publication of the Infectious Diseases Society of America, 1994; 19: 454-462.

40. Hosoya M, Shigeta S, Nakamura K. & De Clercq E. Inhibitory effect of selected antiviral compounds on measles (SSPE) virus replication in vitro. *Antiviral Res.* 1989; 12: 87-97.

41. Cherry J.D. Measles. In : Feigin RD, Cherry JD, editors. *text-book of pediaterics infectious diseases.*, 4th ed philadelphia: WB Saunders: 1998.p. 2054-2074.

42. Jen J, Laughlin M, Chung C, Heft S, Affrime M.B, Gupta S.K, Glue P. et al. (2002) Ribavirin dosing in chronic hepatitis C: application of population pharmacokinetic-pharmacodynamic models. *Clin. Pharmacol. Ther.* 2002; 72: 349-361.

43. Takaki S, Tsubota A, Hosaka T, Akuta N, Someya T, Kobayashi M. et al. Factors contributing to ribavirin dose reduction due to anemia during interferon alfa2b and ribavirin combination therapy for chronic hepatitis C. *ter Meulen, V. & Carter, M.J. (1984) Measles virus persistency and disease. Prog. Med. Virol.* 2004; 30: 44-61.

44. Mosmann T. Rapid colorimetric assay for cellular growth and survival: application to proliferation and cytotoxicity assays. *J. Immunol. Methods* 1983; 65: 55-63.

45. Andrighetti-Frohner C.R, Antonio R.V, Creczynski-Pasa T.B, Barardi C.R. & Simoes C.M. Cytotoxicity and potential antiviral evaluation of violacein produced by *Chromobacterium violaceum*. *Mem. Inst. Oswaldo Cruz* 2003; 98: 843-848.

46. Vietinck A.J. & Vanden-Berghe D.A. Antiviral activity of 3-methoxyflavones. *Proceeding clinical biology research* 1991; 213: 537-540.

47. Simoes C.M, Amoros M. & Girre L. Mechanism of antiviral activity of triterpenoid saponins. *Phytother Res* 1999; 13: 323-328.

48. Semple S.J, Pyke S.M, Reynolds G.D. & Flower R.L. In vitro antiviral activity of the anthraquinone chrysophanic acid against poliovirus. *Antiviral Res.* 2001; 49: 169-178.

49. Li Y.L, Ma S.C, Yang Y.T, Ye S.M. & but P.P. Antiviral activities of flavonoids and organic acid from *Trollius chinensis* Bunge. *J Ethnopharmacol* 2002; 79: 365-368.

50. Smee D.F, Morrison A.C, Barnard D.L. & Sidwell R.W. Comparison of colorimetric, fluorometric, and visual methods for determining anti-influenza (H1N1 and H3N2) virus activities and toxicities of compounds. *J. Virol. Methods* 2002; 106: 71-79.

51. Ortac Ersoy E, Tanriover M.D, Ocal S, Ozisik L, Inkaya C. & Topeli A. Severe measles pneumonia in adults with respiratory failure: role of ribavirin and high-dose vitamin A. *Clin Respir J* 2016; 10: 673-675.

52. Wray S.K, Gilbert B.E & Noall M.W. Mode of action of ribavirin: effect of nucleotide pool alterations on influenza virus ribonucleoprotein synthesis, Noall MW, et al. *Antiviral Res* 1985; 5: 29-37.

53. Thomas B, Beard S, Jin L, Brown K.E. & Brown D.W. Development and evaluation of a real-time PCR assay for rapid identification and semi-quantitation of measles virus. *J. Med. Virol* 2007; 79: 1587-1592.

54. Hummel K.B, Lowe L, Bellini W.J. & Rota P.A. Development of quantitative gene-specific real-time RT-PCR assays for the detection of measles virus in clinical specimens. *Virol. Methods* 2006; 132: 166-173.

55. Mackay I.M, Arden K.E. & Nitsche A. Real-time PCR in virology. *Nucleic Acids Res* 2002; 30: 1292-1305.

56. Griffin D. Measles virus. In: Fields BN, Knipe D.M, and Howley P.M, eds. *Fields Virology*. Philadelphia: Wolters Kluwer Health/ Lippincott Williams & Wilkins, 2007; Vol 2, 1551–1585.